Phytochemistry 209 (2023) 113620

Contents lists available at ScienceDirect

Phytochemistry

journal homepage: www.elsevier.com/locate/phytochem

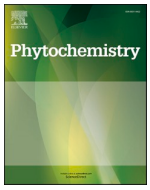

Spatial localization of monoterpenoid indole alkaloids in *Rauvolfia tetraphylla* by high resolution mass spectrometry imaging

Marcus Daniel Brandbjerg Bohn Lorensen [a], Nanna Bjarnholt [b], Benoit St-Pierre [c], Sarah Heinicke [d], Vincent Courdavault [c], Sarah O'Connor [d], Christian Janfelt [a,*]

[a] Department of Pharmacy, Faculty of Health and Medical Sciences, University of Copenhagen, Universitetsparken 2, 2100, Copenhagen, Denmark
[b] Plant Biochemistry Laboratory and Copenhagen Plant Science Center, Department of Plant and Environmental Sciences, University of Copenhagen, 1871, Frederiksberg, Denmark
[c] Université de Tours, EA2106 Biomolécules et Biotechnologies Végétales, 37200, Tours, France
[d] Max Planck Institute for Chemical Ecology, Department of Natural Product Biosynthesis, Hans-Knöll-Straße 8, 07745, Jena, Germany

ARTICLE INFO

Keywords:
Mass spectrometry imaging
MALDI-MSI
DESI-MSI
Rauvolfia tetraphylla
Reserpine
Monoterpenoid indole alkaloids

ABSTRACT

Monoterpenoid indole alkaloids (MIAs) are a large group of biosynthetic compounds, which have pharmacological properties. One of these MIAs, reserpine, was discovered in the 1950s and has shown properties as an anti-hypertension and anti-microbial agent. Reserpine was found to be produced in various plant species within the genus of *Rauvolfia*. However, even though its presence is well known, it is still unknown in which tissues *Rauvolfia* produce reserpine and where the individual steps in the biosynthetic pathway take place.

In this study, we explore how matrix assisted laser desorption ionization (MALDI) and desorption electrospray ionization (DESI) mass spectrometry imaging (MSI) can be used in the investigation of a proposed biosynthetic pathway by localizing reserpine and the theoretical intermediates of it. The results show that ions corresponding to intermediates of reserpine were localized in several of the major parts of *Rauvolfia tetraphylla* when analyzed by MALDI- and DESI-MSI. In stem tissue, reserpine and many of the intermediates were found compartmentalized in the xylem. For most samples, reserpine itself was mainly found in the outer layers of the sample, suggesting it may function as a defense compound.

To further confirm the place of the different metabolites in the reserpine biosynthetic pathway, roots and leaves of *R. tetraphylla* were fed a stable-isotope labelled version of the precursor tryptamine. Subsequently, several of the proposed intermediates were detected in the normal version as well as in the isotope labelled versions, confirming that they were synthesized *in planta* from tryptamine. In this experiment, a potential novel dimeric MIA was discovered in leaf tissue of *R. tetraphylla*.

The study constitutes to date the most comprehensive spatial mapping of metabolites in the *R. tetraphylla* plant. In addition, the article also contains new illustrations of the anatomy of *R. tetraphylla*.

1. Introduction

Rauvolfia tetraphylla L. (Apocynaceae), also known as 'Devil Pepper' and 'Be Still Tree', is a plant which has received attention due to its ability to produce compounds with medical properties. *R. tetraphylla* appears as a combination between a tree and a shrub that can grow up to the height of 1.8 m (Gupta et al., 2012; Iqbal et al., 2013; Verma et al., 2012). *R. tetraphylla* has been used in traditional medicine in several areas of India, often as a substitute for *Rauvolfia serpentine* (Mahalakshmi et al., 2019). Traditional medicine made from *R. tetraphylla* has been used to treat headache (Ganesh and Sudarsanam, 2013), skin diseases, snake bite, insect bite (Kumar et al., 2018), stomachache (Malaiya, 2016), blood pressure (Babu et al., 2010), and diarrhea (Morshed and Nandni, 2012). Indeed, *Rauvolfia* sp. Synthesize secondary metabolites known as monoterpenoid indole alkaloids (MIAs) displaying significant biological activities. MIAs are a large group of biosynthetically related metabolites, with *Rauvolfia* sp. Known for production of MIAs like reserpine (Muller et al., 1952), ajmaline (Stöckigt et al., 2007), alstonine (Elisabetsky and Costa-Campos, 2006) and yohimbine (Kumar et al., 2016) used as drugs. MIAs in general have a wide variety of complex

* Corresponding author.
E-mail address: christian.janfelt@sund.ku.dk (C. Janfelt).

https://doi.org/10.1016/j.phytochem.2023.113620
Received 22 November 2022; Received in revised form 20 February 2023; Accepted 22 February 2023
Available online 1 March 2023

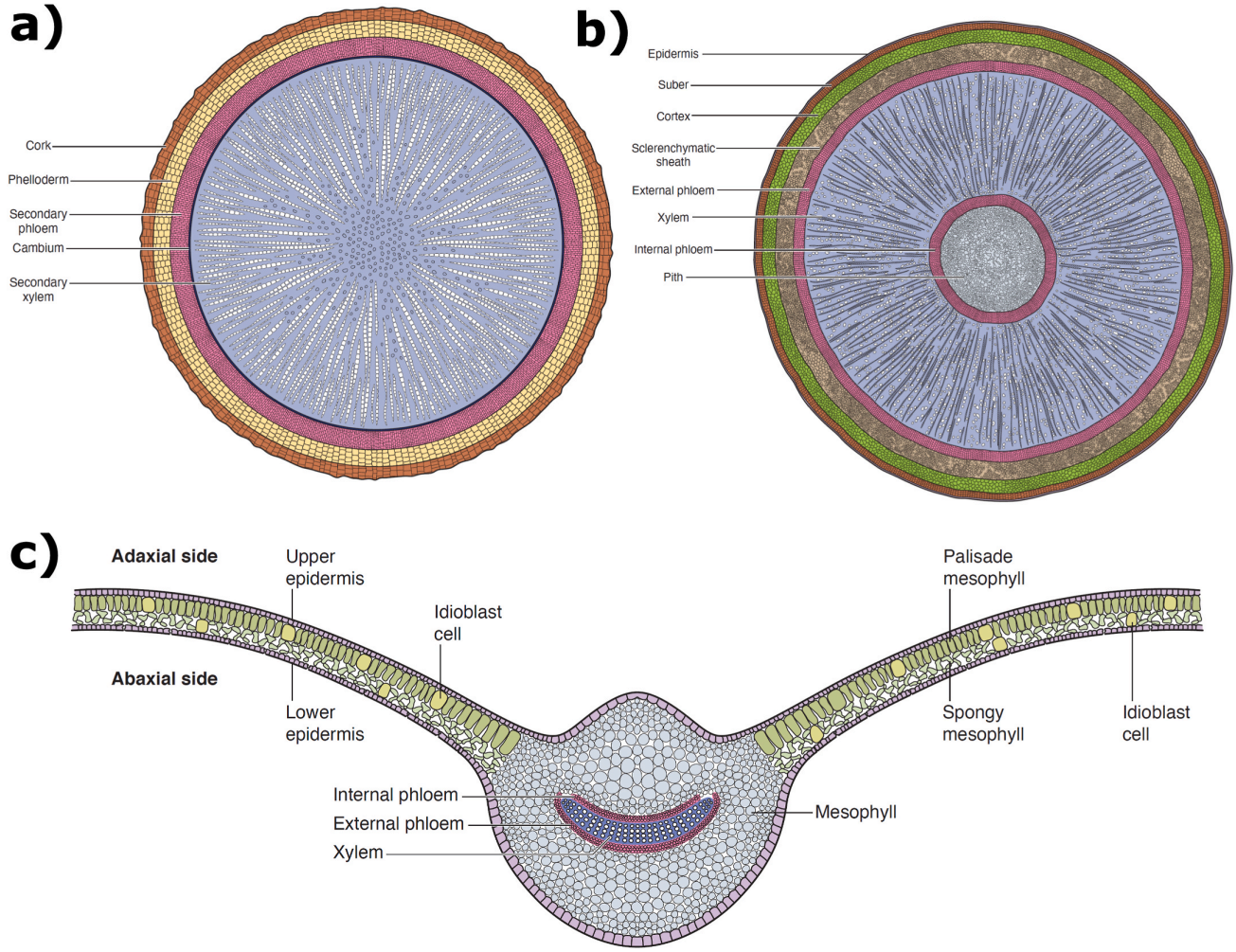

Fig. 1. Illustrations of the anatomy of the imaged parts of R. tetraphylla. a) root. b) stem. c) leaf. A corresponding drawing of the berry is found in Fig. S2.

structures, which make them challenging to produce by conventional chemical synthesis at industrial scales. Exploitation of these compounds mainly relies on extraction from plant tissue which is complicated since many MIAs are produced in very low levels *in planta* (Deshmukh et al., 2012; Miettinen et al., 2014).

MIAs result from long and complex biosynthetic pathways that also exhibit a complex organization at both the cellular and subcellular levels (de Bernonville et al., 2015; Pan et al., 2016; Yamamoto et al., 2019). They have previously been localized in the tissues of the well-known MIA producing plant *Catharanthus roseus* (also of the Apocynaceae family) using immunostaining (St-Pierre et al., 1999) and MALDI-MSI (Yamamoto et al., 2016).

All MIAs derive from the same common precursor, strictosidine, which is synthesized by strictosidine synthase from secologanin and tryptamine (St-Pierre et al., 2013; Treimer and Zenk, 1979). Secologanin derives from the seco-iridoid pathway, which has been thoroughly studied in *C. roseus*. The seco-iridoid pathway has been shown to take place initially in internal phloem-associated parenchyma cells and finalized in epidermis cells (Burlat et al., 2004; Miettinen et al., 2014), where strictosidine synthase is located (St-Pierre et al., 1999). This implies that strictosidine precursors are being transported to the epidermal cells. However, more recent studies have found that strictosidine accumulates in idioblasts and laticifer cells in *C. rosues* (Yamamoto et al., 2016, 2019), which suggest that it is transported there from the epidermis. Many post-strictosidine steps have been discovered in *C. roseus*; in *Rauvolfia* sp., however, only the ajmaline pathway has been investigated (Dang et al., 2017, 2018).

Among the pathways beyond strictosidine that have still not been explored are the biosynthetic pathways of reserpine and rescinnamine in *R. tetraphylla*. Reserpine and rescinnamine were isolated for the first time in 1952 and 1954, respectively (Klohs et al., 1954; Muller et al., 1952). They share similar structure and have both been shown to have sedative and antihypertension effects (Bakris and Frohlich, 1989; Fife et al., 1960). Reserpine has also been shown to possess antimicrobial properties (Mullin et al., 2004; Stavri et al., 2007; Vaou et al., 2021). A proposed biosynthetic pathway for reserpine and rescinnamine, based on previously elucidated MIA pathways (O'Connor and Maresh, 2006) is shown in. Fig. 2 Intermediates shown in the proposed biosynthetic pathway are named RPI 2–7.

To gain insights into reserpine and rescinnamine metabolism, more information is needed about the spatial distribution of the different metabolites. A mass spectrometry based technique known as Mass Spectrometry Imaging (MSI) constitute a powerful tool to analyze the spatial location of reserpine, rescinnamine and their intermediates *in situ* (Bjarnholt et al., 2014; Boughton et al., 2016). MSI enables mass-specific imaging of numerous compounds in a sample in one experiment. It is performed by rastering a sample below an ionization spot such that a mass spectrum is acquired in every point on the samples. Subsequently,

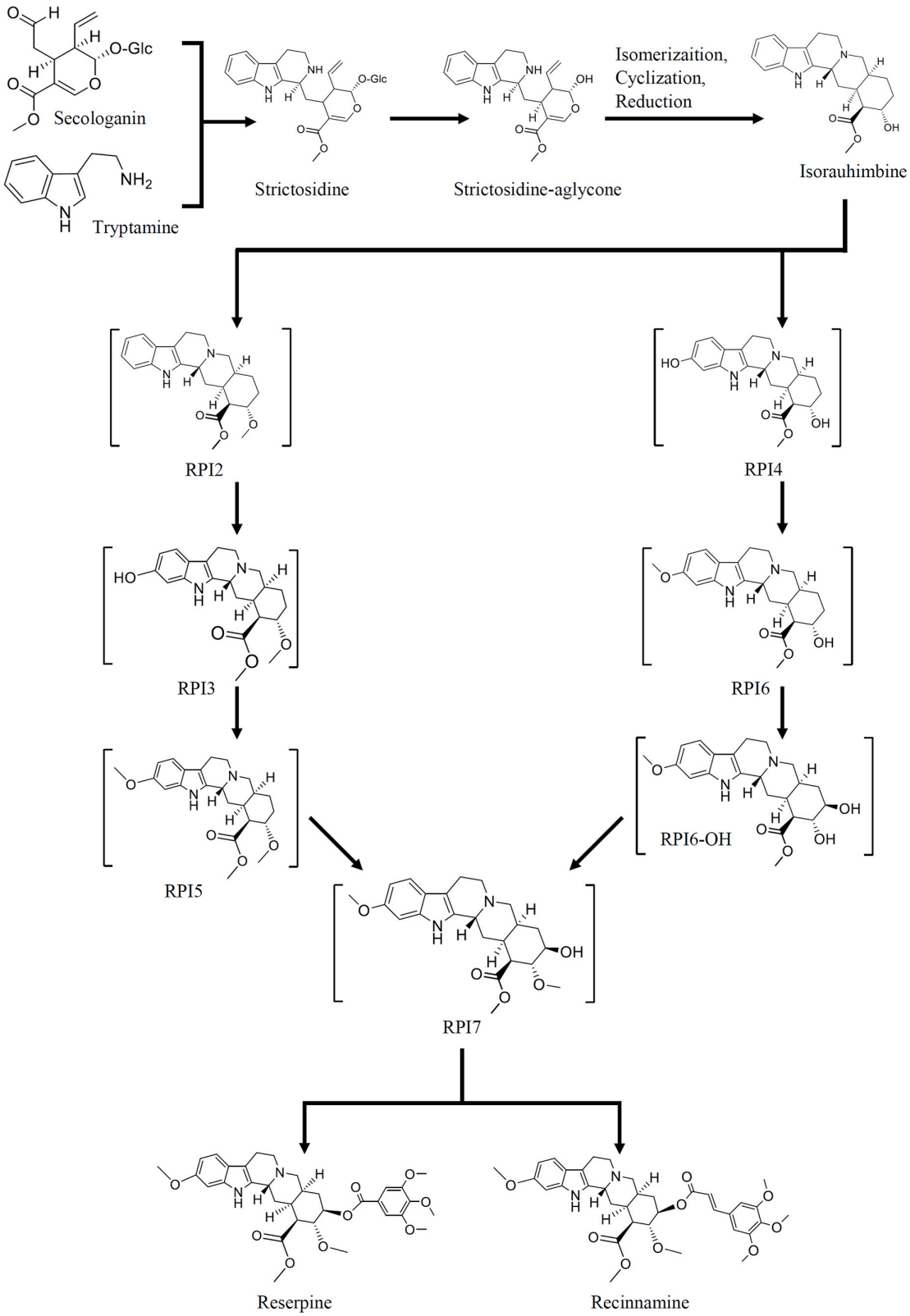

Fig. 2. Theoretical biosynthetic pathway of reserpine and rescinnamine. The brackets indicate which intermediates should be considered as tentative.

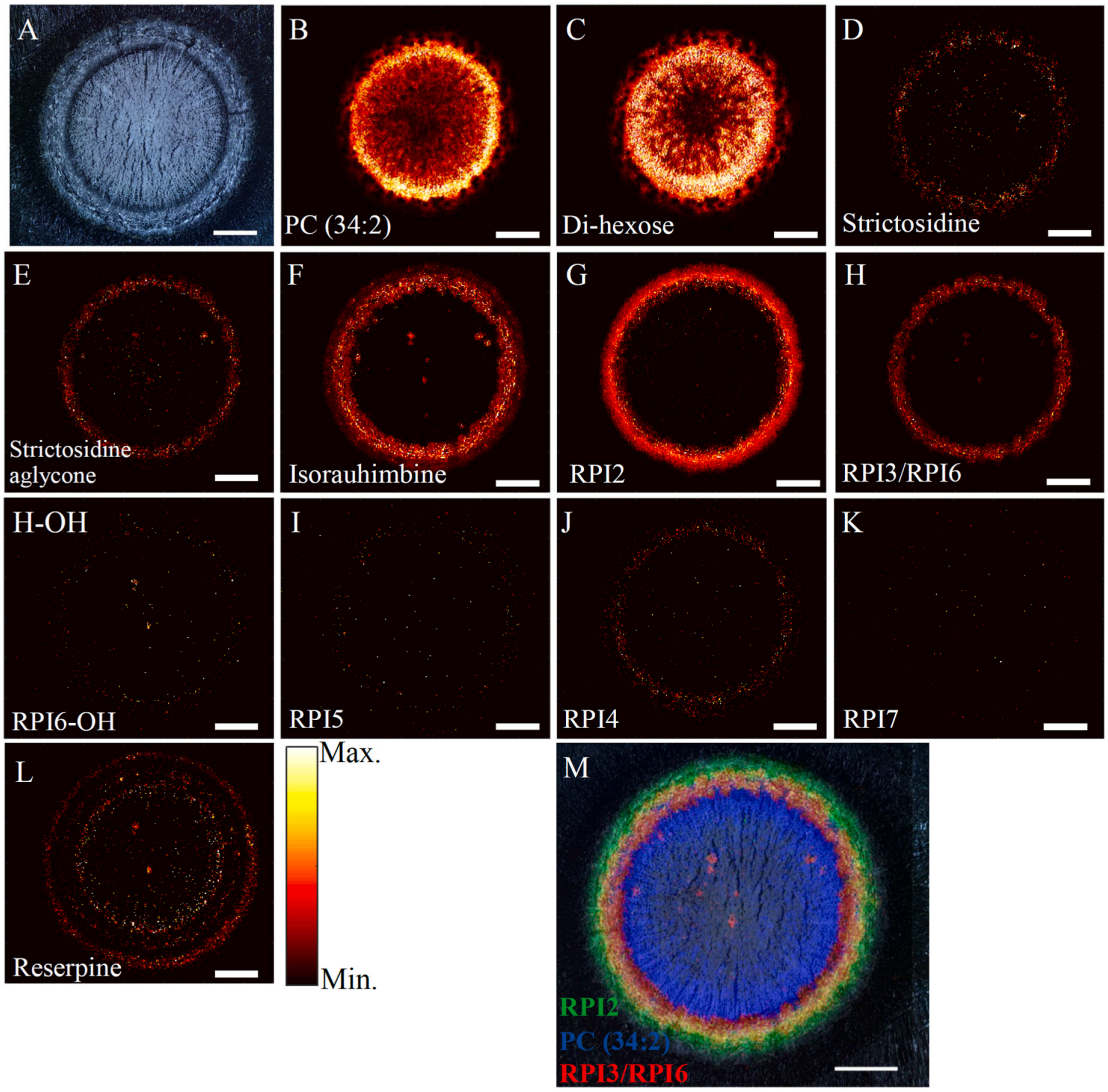

Fig. 3. MALDI-MS images of R. tetraphylla root tissue. (A) Microscope image. (B) PC (34:2). (C) Di-hexose. (D) Strictosidine. (E) Strictosidine aglycone. (F) Isorauhimbine. (G) RPI2. (H) RPI3/RPI6. (H–OH) RPI6-OH. (I) RPI5. (J) RPI4. (K) RPI7. (L) Reserpine. (M) Co-localization RGB image showing RPI3/PRI6 in red, RPI2 in green and PC(34:2) in blue. The pixel size is 20 μm. Scale bars: 1 mm. (For interpretation of the references to color in this figure legend, the reader is referred to the Web version of this article.)

heatmaps of ion intensities can be extracted for each compound of interest, with every recorded mass spectrum corresponding to a pixel in the final image. In this study, both Matrix Assisted Laser Desorption Ionization (MALDI)-MSI and Desorption Electrospray Ionization (DESI)-MSI was used. In brief, MALDI-MSI enables spatial resolution as high as 1–5 μm while DESI-MSI typically enables spatial resolution of 50 μm or lower. MALDI-MSI uses a UV laser for ionization and requires application of a layer of UV-absorbing matrix molecules onto the sample, while DESI uses solvent spray for ionization and can analyze the samples directly after sample preparation such as cryo-sectioning or imprinting (Feenstra et al., 2017; Li et al., 2016). MSI has been utilized to propose a biosynthetic pathway in *Linum usitatissimum* seeds (Dalisay et al., 2015) based on co-localization of metabolites and transcripts. In *C. roseus*, MALDI-MSI was used on leaves (Yamamoto et al., 2019) and stem tissue (Yamamoto et al., 2016) to decipher MIA pathway organization with a spatial resolution of 10–20 μm. DESI-MSI was used to study MIAs in leaf, stem, root and fruit tissue of *R . Tetraphylla* at a spatial resolution of 250 μm (Kumara et al., 2019).

In the present study, the MIA distribution in *R. tetraphylla* is further investigated by high-resolution MALDI-MSI in combination with DESI-MSI, focusing on the biosynthetic pathways of reserpine and rescinnamine. The proposed pathway was investigated in leaf, stem, root and fruit tissue of *R. tetraphylla*. Compared to the previous MSI study of *R. tetraphylla*, imaging was performed at a significantly higher spatial resolution (15 or 20 μm), which enabled much more detailed visualization, including imaging of cross sections of leaves.

2. Results and discussion

The present study represents a comprehensive analysis of the distribution of reserpine and theoretical intermediates of reserpine biosynthesis in the main structures of the *R. tetraphylla* plant, including root, stem, leaf and fruit tissue. Most of the imaging experiments have been carried out by MALDI-MSI due to its superior spatial resolution, but the lateral distribution of the metabolites in leaf was investigated by DESI-MSI due to its capabilities for direct analysis of imprints on porous

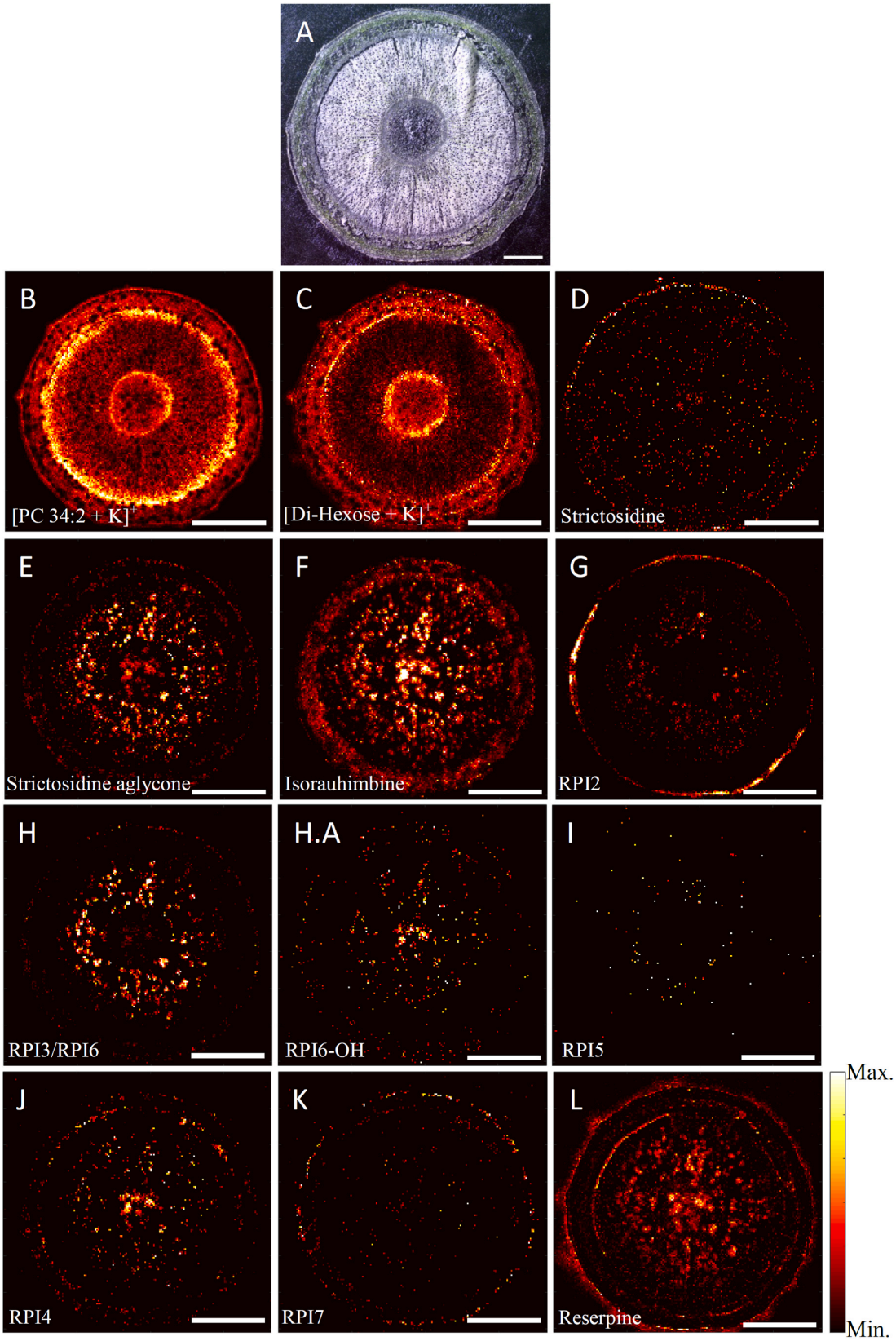

Fig. 4. MALDI-MS images of R. tetraphylla primary stem tissue. (A) Microscope image. (B) PC (34:2). (C) Di-hexose. (D) Strictosidine. (E) Strictosidine aglycone. (F) Isorauhimbine. (G) RPI2. (H) RPI3/RPI6. (H.A) RPI6-OH. (I) RPI5. (J) RPI4. (K) RPI7. (L) Reserpine. The pixel size is 20 μm. Scale bars: 2 mm.

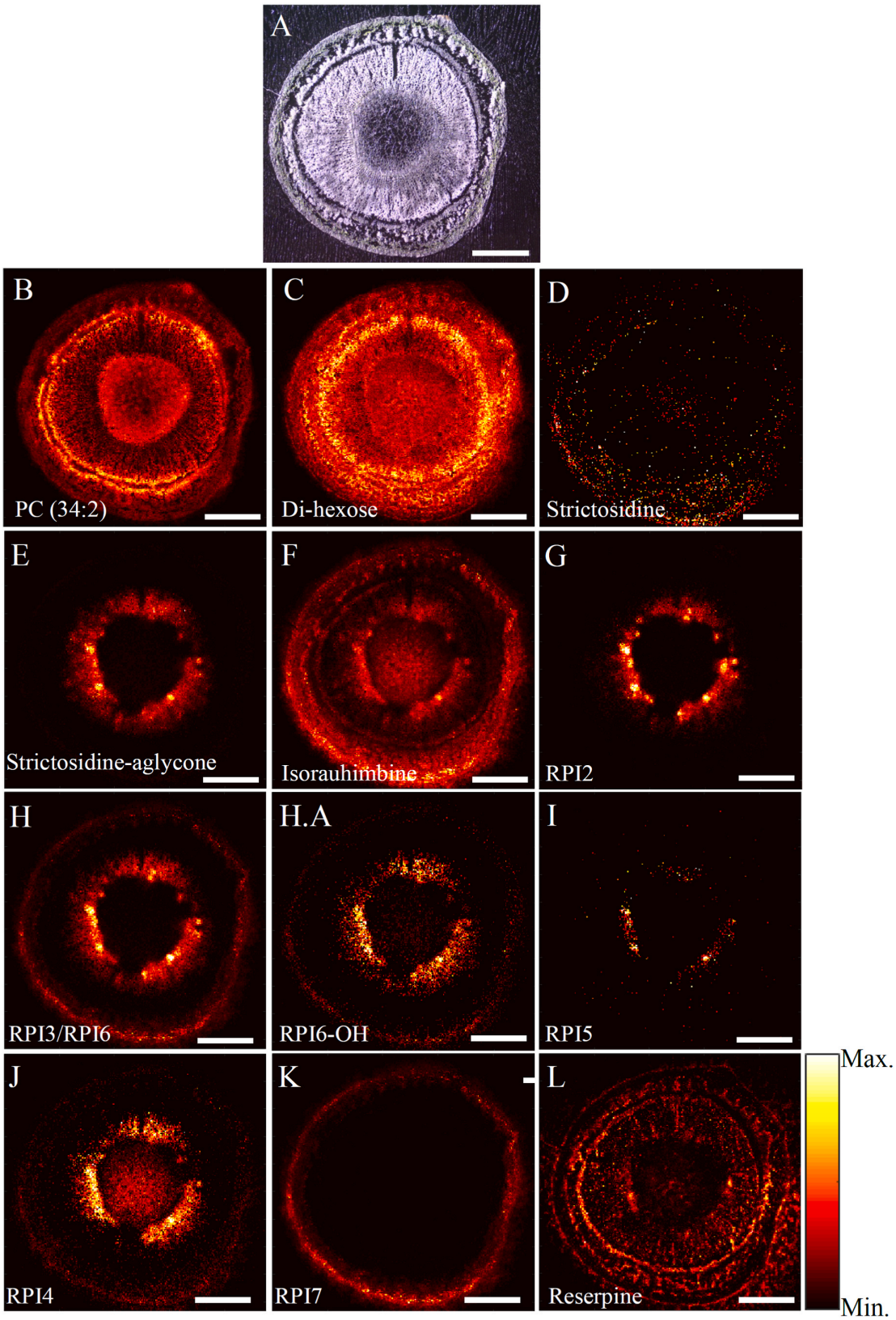

Fig. 5. MALDI-MS images of R. tetraphylla secondary stem tissue. (A) Microscope image. (B) PC (34:2). (C) Di-hexose. (D) Strictosidine. (E) Strictosidine aglycone. (F) Isorauhimbine. (G) RPI2. (H) RPI3/RPI6. (H.A) RPI6-OH. (I) RPI5. (J) RPI4. (K) RPI7. (L) Reserpine. The pixel size is 20 μm. Scale bars: 1 mm.

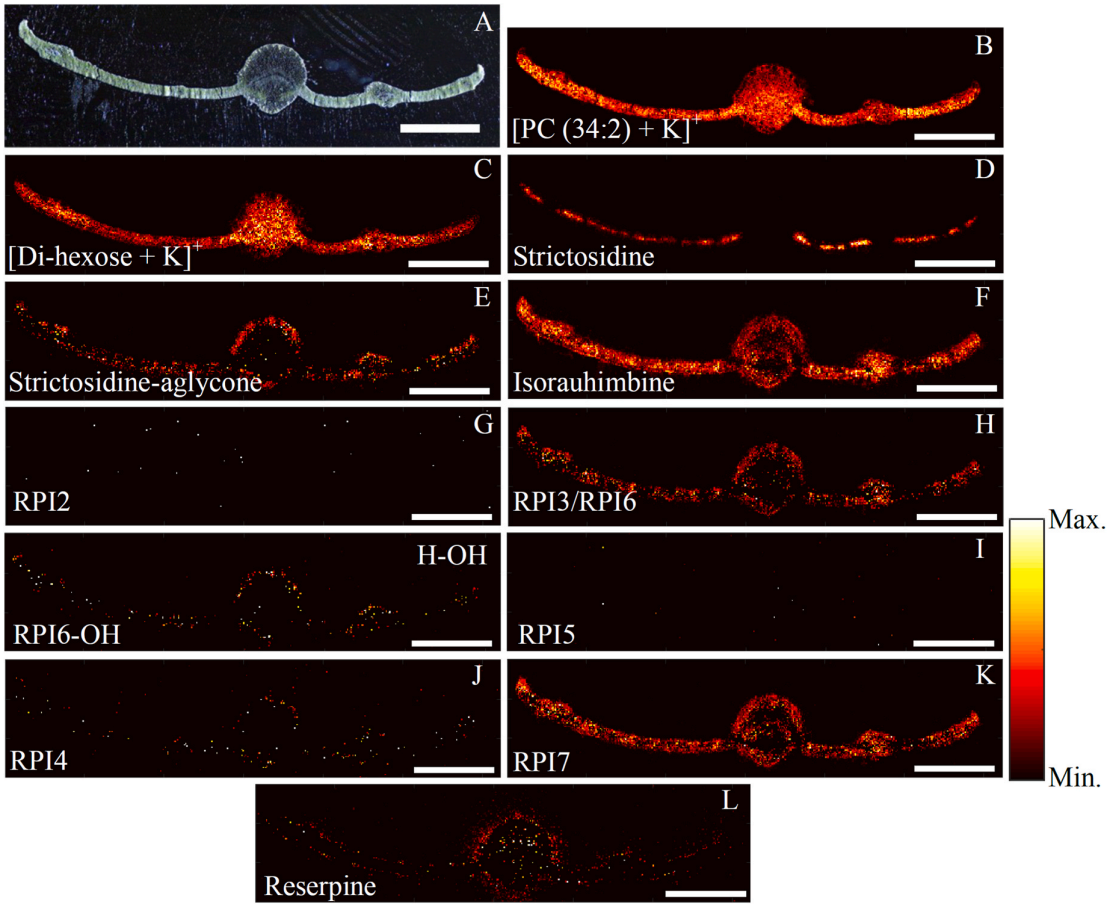

Fig. 6. MALDI-MS images a cross section of R. tetraphylla young leaf tissue. (A) Microscope image. (B) PC(34:2). (C) Di-hexose. (D) Strictosidine. (E) Strictosidine aglycone. (F) Isorauhimbine. (G) RPI2. (H) RPI3/RPI6. (H–OH) RPI6-OH. (I) RPI5. (J) RPI4. (K) RPI7. (L) Reserpine. The pixel size is 15 μm. Scale bars: 1 mm.

PTFE surfaces. MALDI- as well as DESI-MSI was carried out on an Orbitrap mass spectrometer providing high resolution MS analysis with a mass accuracy of 2 ppm, excluding most compounds of similar, but not identical masses.

To aid with interpretation of the presented MSI data, illustrations are provided in Fig. 1, which show the anatomy of root, stem and leaf material of *R. tetraphylla*. These illustrations were inspired by the several studies of the anatomy of *Rauvolfia* sp. And other members of Apocynaceae (Baratto et al., 2010; Court et al., 1957; Metcalfe and Chalk, 1950). Compounds included in the reserpine and rescinnamine pathway in Fig. 2 have been imaged by MALDI-MSI and DESI-MSI in root, stem, and leaf tissues as shown in Figs. 3–9. The identification of the compounds is based on the accurate mass of the compounds, but some of these compounds have one or more known isomers, which in principle could contribute to the imaged signals. These potentially interfering compounds have been listed in Table 1. For each MSI experiment, an image of phosphatidylcholine 34:2 (PC (34:2)) or di-hexose is included to show the contour of the analyzed tissue. Rescinnamine was not detected in any tissue of *R. tetraphylla* and is therefore not included in any of the figures. The findings from the MSI experiments have been summarized in Table 2, which provides an overview of the parts of the plant in which reserpine and the intermediates of reserpine and rescinnamine were detected. Additional experiments were made on immature and mature fruits, and the results from these experiments are found in the supporting information.

It should be noted that results from MSI experiments are generally to be considered of qualitative nature. From the reported images it can thus only be inferred where the compounds were observed, but not in which quantity. Nor can the relative abundances of different compounds be assessed, as different compounds may have different ionization efficiencies.

2.1. Root tissue

MALDI-MS images of a cross section of a *R. tetraphylla* root is found in Fig. 3. MALDI-MS images of PC (34:2) and di-hexose (Fig. 3B-C) show that PC 34:2 and di-hexose are not observed in the entire root tissue, but they give an indication of the xylem tissue. Most reserpine/rescinnamine intermediates are observed in the secondary phloem. However, as is more clearly seen in the overlaid image in Fig. 3M, RPI2 is observed in the phelloderm compared to the other intermediates. From the merged MS image of RPI2, RPI3 and PC 34:2, it is observed that RPI2 (Green) and RPI3 (Red) are localized in two different layers (the phloem and the phelloderm), which could indicate some transport of either RPI2 or RPI3 and the rest of the intermediates between the two layers. The intermediates RPI5 and RPI7 (Fig. 3 I & K) were not detected. This could indicate that instead of accumulating, the compounds are rapidly further metabolized, thus not reaching high enough amounts to be detected. Root tissue was the only tissue where RPI7 was not detected. The reason could be that its further conversion into reserpine and/or rescinnamine is particularly efficient in the roots, preventing its accumulation. Reserpine is mostly present in the phloem, phelloderm, cork and around the xylem. In the study by Kumara et al. (2019), MIAs are also observed in what is referred to as cortex, which is similar to the area of secondary

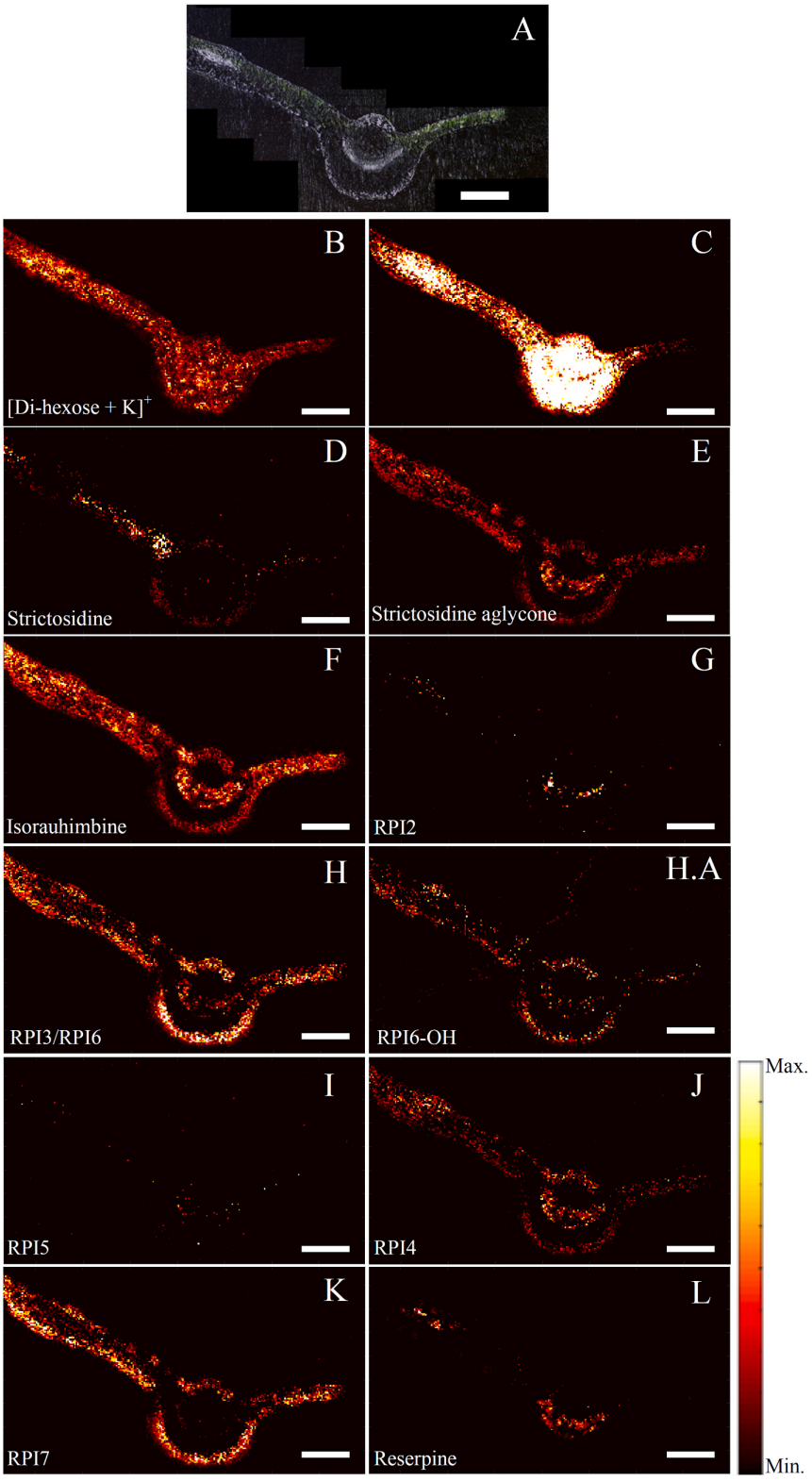

Fig. 7. MALDI-MS images of R. tetraphylla old leaf tissue. (A) Microscope image. (B) PC (34:2). (C) Di-hexose. (D) Strictosidine. (E) Strictosidine aglycone. (F) Isorauhimbine. (G) RPI2. (H) RPI3/RPI6. (H.A) RPI6-OH. (I) RPI5. (J) RPI4. (K) RPI7. (L) Reserpine. The pixel size is 20 μm. Scale bars: 1 mm.

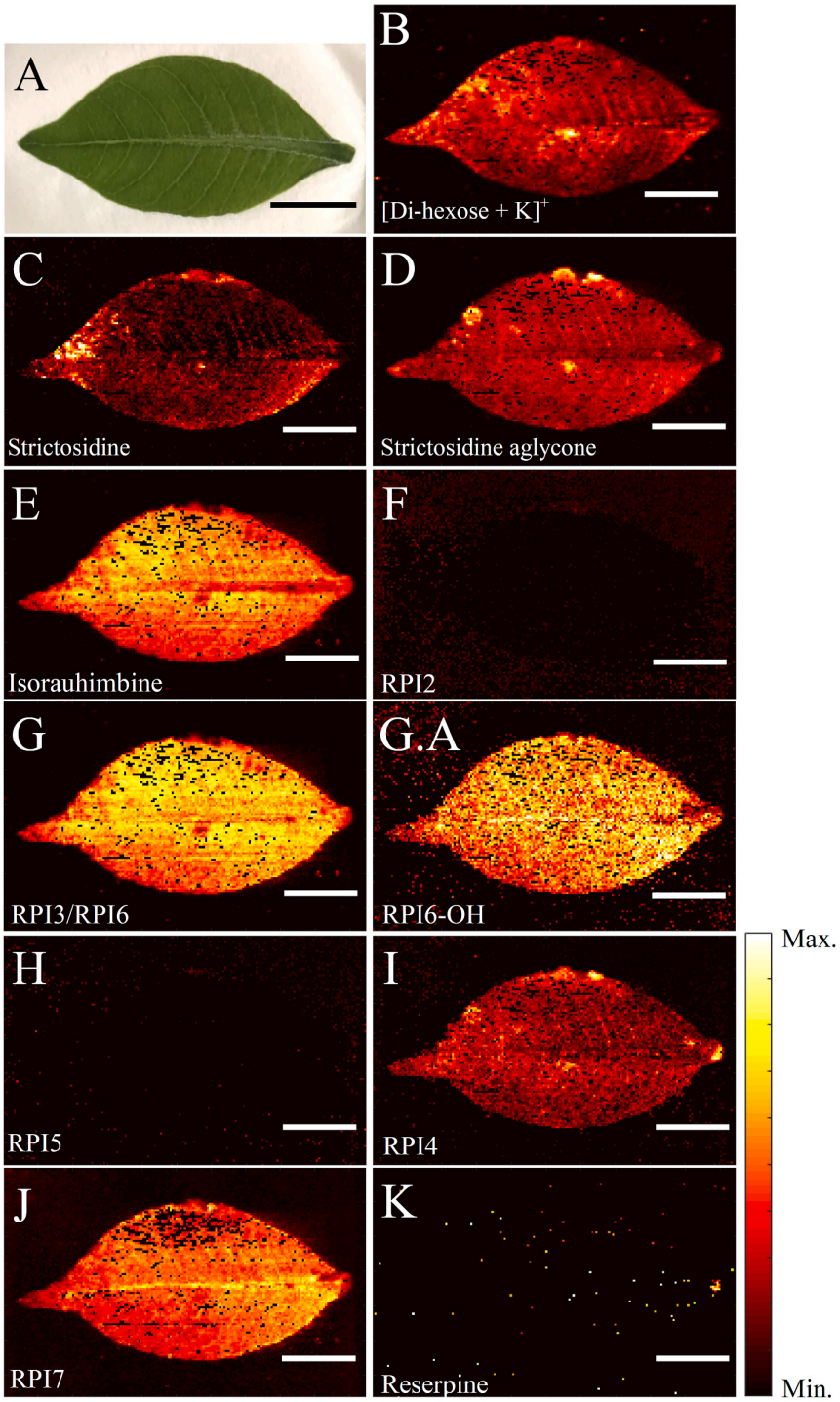

Fig. 8. DESI-MS images of the PTFE imprint of a young leaf from R. tetraphylla. (A) Photo of leaf prior to imprinting. (B) Di-hexose. (C) Strictosidine. (D) Strictosidine aglycone. (E) Isorauhimbine. (F) RPI2. (G) RPI3/RPI6. (G.A) RPI6-OH. (H) RPI5. (I) RPI4. (J) RPI7. (K) Reserpine. The pixel size is 300 μm. Scale bars: 10 mm.

phloem and phelloderm. These findings suggest that the biosynthetic pathway of reserpine and rescinnamine occurs in the cortex of the root.

2.2. Stem tissue

Fig. 4 shows MALDI–MS images of primary stem tissue of *R. tetraphylla*, and Fig. 5 shows the corresponding images of secondary stem tissue. In the primary stem tissue, the reserpine and rescinnamine intermediates are observed in small compartments in the pith and xylem region, indicating existence of specialized cells responsible for MIA production in primary stem tissue. In addition to this, RPI2 was also observed in the epidermal layer of primary stem tissue (Fig. 4G), which

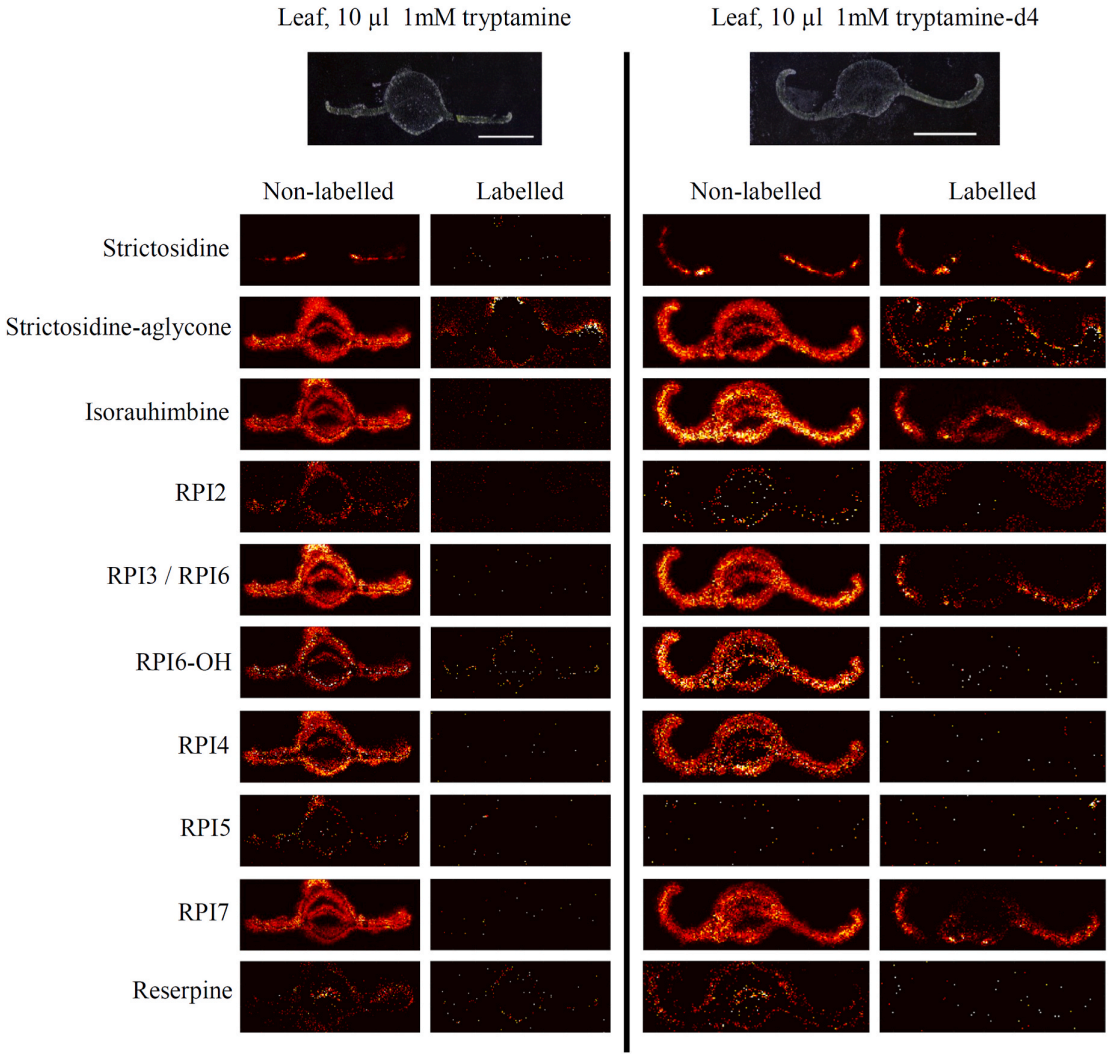

Fig. 9. MALDI-MS images showing isotope labelled reserpine and its intermediates in leaf cross-sections of R. tetraphylla. MS images of two leaves are shown. Leaf A was administered 10 µl 1 mM tryptamine and Leaf B was administered 10 µl 1 mM tryptamine-d4. The MS images are divided into two groups, the unlabeled and labelled. *m/z* values of the labelled and unlabeled masses can be viewed in Table 1. The pixel size is 20 µm. Scale bars: 1 mm.

is in contrast to secondary stem tissue where it was only observed in small compartments close to the internal phloem (Fig. 5G). In general, secondary stem tissue appears quite distinct from the primary stem, as most intermediates are localized around the pith and internal phloem in secondary stem (Fig. 5). However, as seen for strictosidine aglycone, RPI2, 3 and 6 (Fig. 4E, G and H), there seem to be smaller compartments close to or within the internal phloem in primary stem, which could suggest that it has similar specialized cells.

Yamamoto et al. (2016) analyzed stem tissue of *C. roseus* and found MIAs to be present around the vascular bundle, idioblast cells and laticifer cell by MSI. However, analysis of stem tissue from *Rauvolfia sellowii* found idioblast cells present in cortex and pith and laticifer cells only present in the pith (Baratto et al., 2010). Therefore, it is unlikely that the MIA compartments in xylem seen in Figs. 4 and 5 are due to idioblast or laticifer cells (assuming that the anatomy of *R. tetraphylla* is similar to the one of *R. sellowii*).

Yamamoto et al. (2016) found the majority of strictosidine present in the idioblast and laticifer cells in the stem tissue of *C. roseus*. However, while in the present study strictosidine was detected in both primary and secondary stem tissue, due to highly scattered and low intensity it is not possible to conclude specifically where the molecule is localized (Figs. 4D and 5D). RPI5 was not detected in primary stem tissue, however in the secondary stem tissue it was observed around the internal phloem, like the other intermediates. RPI7 is the only intermediate not observed in the xylem, phloem or pith and is only observed in the epidermis/suber area of both primary and secondary stem tissue. This could mean that the last step of the reserpine/rescinnamine pathway takes place in the epidermis/suber; however, more evidence for the pathway is required before this can be concluded. In primary stem tissue, reserpine was observed in compartments in pith and xylem as the intermediates. In secondary tissue reserpine was observed in the xylem, however not in compartments like in the primary tissue. In both primary and secondary stem tissue, reserpine was also observed in the epidermal layer and in external phloem/cortex. The reason why it is present in the epidermal cells could be that it serves as a defense compound, something which is well in line with its antimicrobial effects previously described (Bakris and Frohlich, 1989; Mullin et al., 2004; Stavri et al., 2007; Vaou et al., 2021). Given its presence in external phloem, it could be that it is being transported via these cells, however no evidence for transporters of reserpine in this tissue have been documented before.

Table 1
Reserpine and rescinnamine intermediates.

Name	Molecular formula	Monoisotopic mass	$[M+H]^+$	$[M+Na]^+$	$[M+K]^+$	Known isomers
Strictosidine	$C_{27}H_{34}N_2O_9$	530.22643	531.23371	553.21565	569.18959	
Strictosidine aglycone	$C_{21}H_{24}N_2O_4$	368.17361	369.18088	391.16283	407.13677	
Isorauhimbine	$C_{21}H_{26}N_2O_3$	354.19434	355.20162	377.18356	393.15750	Rauhimbine[1,2] Yohimbine[3] α-yohimbine[4] Acetylnorajmaline[5]
RPI2	$C_{22}H_{28}N_2O_3$	368.20999	369.21727	391.19921	407.17315	
RPI3	$C_{22}H_{28}N_2O_4$	384.20491	385.21218	407.19413	423.16807	RPI6
RPI4	$C_{21}H_{26}N_2O_4$	370.18926	371.19653	393.17848	409.15242	18-Hydroxyepialloyohimbine[3]
RPI5	$C_{23}H_{30}N_2O_4$	398.22056	399.22783	421.20978	437.18372	
RPI6	$C_{22}H_{28}N_2O_4$	384.20491	385.21218	407.19413	423.16807	RPI3
RPI6-OH	$C_{22}H_{28}N_2O_4$	400.19982	401.20710	423.18904	439.16298	Reserpic acid
RPI7	$C_{23}H_{30}N_2O_5$	414.21547	415.22275	437.20469	453.17863	Seredine[6,7] Reserpic acid methyl ester[6,7]
Reserpine	$C_{33}H_{40}N_2O_9$	608.27338	609.28066	631.26260	647.23654	
Rescinamine	$C_{35}H_{42}N_2O_9$	634.28903	635.29631	657.27825	673.25219	
Strictosidine-d4	$C_{27}H_{30}N_2O_9D_4$	534.25153	535.25881	557.24075	573.21469	
Strictosidine aglycone-d4	$C_{21}H_{20}N_2O_4D_4$	372.19871	373.20598	395.18793	411.16187	
Isorauhimbine-d4	$C_{21}H_{22}N_2O_3D_4$	358.21944	359.22672	381.20866	397.18260	
RPI2-d4	$C_{22}H_{24}N_2O_3D_4$	372.23509	373.24237	395.22431	411.19825	
RPI3-d4	$C_{22}H_{24}N_2O_4D_4$	388.23001	389.23728	411.21923	427.19317	
RPI4-d4	$C_{21}H_{22}N_2O_4D_4$	374.21436	375.22163	397.20358	413.17752	
RPI5-d4	$C_{23}H_{26}N_2O_4D_4$	402.24566	403.25293	425.23488	441.20882	
RPI6-d4	$C_{22}H_{24}N_2O_4D_4$	388.23001	389.23728	411.21923	427.19317	
RPI7-d4	$C_{23}H_{26}N_2O_5D_4$	418.24057	419.24785	441.22979	457.20373	
Reserpine-d4	$C_{33}H_{36}N_2O_9D_4$	612.29848	613.30576	635.28770	651.26164	
Vincristine-like compound	$C_{46}H_{56}N_4O_{10}$	824.39964	825.40692	847.38886	863.36280	
Vincristine-like compound-d4	$C_{46}H_{52}N_4O_{10}D_4$	828.42474	829.43202	851.41396	867.38790	

2.3. Leaf tissue

Leaf tissues were analyzed by MALDI-MSI and DESI-MSI. MALDI was used to analyze cross sections of young and old leaf tissue (Figs. 6 and 7, respectively), while DESI was used to analyze abaxial imprints of young and old leaf tissue on PTFE (Fig. 8 and Fig. S1, respectively). In both DESI and MALDI-MS-images of young and old leaf tissue, most of the reserpine and rescinnamine intermediates were detected. The DESI-MS image of strictosidine (Fig. 8C) shows its presence in most of the leaf tissue except the veins. This is seen more clearly in the cross section imaged by MALDI (Fig. 6D), where strictosidine was present in the mesophyll area but completely devoid from the midrib and veins. Most MALDI-MS images of old leaf tissue (Fig. 7) showed that strictosidine was observed in the mesophyll area (like in young leaf tissue) but also in the mesophyll close to the epidermis in midrib area. The common theory is that strictosidine is biosynthesized in the epidermis cells in leaf tissue. However, this is also based on early findings in *C. roseus* (St-Pierre et al., 1999), where Yamamoto et al. (2019) found strictosidine not only in epidermis, but also in idioblast cells, laticifer cells as well as spongy and palisade mesophyll. These papers together with the findings in this paper could suggest that strictosidine is being transported across cells. It remains, however, to be proven that strictosidine is biosynthesized in the epidermis of *Rauvolfia* sp. As it is in *C. roseus*.

The next metabolite, strictosidine aglycone, was detected with both DESI and MALDI. Strictosidine aglycone was detected in the midrib and veins of both old and young lead tissue (Figs. 6E and 7E). In old leaf tissue strictosidine aglycone was also detected around the xylem, supposedly in the phloem area (Fig. 7E). This further supports the theory that reserpine biosynthetic intermediates are transported between tissues of *R. tetraphylla*.

RPI2 and RPI5 were not detected by DESI and MALDI in young leaf tissue, but they were detected in old leaf tissue. DESI-MS images of the old leaf tissue show both RPI2 and RPI5 (Fig. S1 F and H) in the midrib and veins. RPI5 was not detected by MALDI, but RPI2 was found in the phloem of the midrib (Fig. 7G). The difference between the DESI and MALDI detection of RPI5 could be ascribed to DESI being more sensitive than MALDI in this instance, perhaps also owing to the sample preparation in the DESI experiments where the soluble leaf contents are extracted into the pores of the PTFE surface.

RPI4 was not detected by MALDI in young leaf tissue, but in the DESI-MS image of young leaf tissue it was detected in both mesophyll, vein and midrib regions. The same distribution of RPI4 in DESI-MS and MALDI-MS images was observed in old leaf tissue. MALDI-MS images of old leaf tissue showed that RPI4 shared the same distribution of strictosidine aglycone, isorauhimbine, RPI3 and RPI6.

DESI-MS and MALDI-MS images of RPI7 show it to be present in the mesophyll tissue in young as well as in old leaves. MALDI-MS images also show RPI7 to be present in the phloem in young leaves (Fig. 6K) but not in the old leaves (Fig. 7K). This could indicate that RPI7 is being converted or transported to other parts of the plant in the young stages of leaf development.

DESI analysis of old and young leaf tissue did not give indications of the spatial location of reserpine. MALDI analysis of young leaf tissue showed presence of reserpine internally in young leaf tissue. However, in some MALDI analyses, reserpine was detected around the midrib, in the epidermal layer (Fig. 6L). In the MALDI-MS images of young leaves, reserpine was also observed outside the tissue area, which might suggest presence of reserpine in the cuticle. The MALDI analysis of old leaf tissue showed the presence of reserpine in the veins and phloem in midribs. This could suggest that reserpine is accumulated in or transported via the phloem in the leaves.

2.4. Fruit tissue

MALDI-MS images of mature and immature fruit cross-sections (Figs. S3 and S4) show that most intermediates were detected in the fruits, primarily in the epidermis or the pedicel. This is in agreement with Kumara et al. (2019) that also found most MIAs in the epidermis of fruits. Strictosidine differs from this pattern as it is observed primarily around the seed and in the pericarp in the immature fruit (Fig. S3D). In the mature fruit tissue, strictosidine was observed in the epidermis tissue similar to the other intermediates (Fig. S4D). RPI2 was faintly observed in some MS images of both the mature and immature fruit tissue around the pedicel; however, due to the inconsistency of its detection, it is

Table 2
Overview of the observed localisations of reserpine andthe different reserpine and rescinnamine intermediates.

Compound	Root	Stem	Leaf	Berry
Strictosidine	✓ Secondary phloem	✓	✓ Mesophyll	✓ Pericarp (immature), epidermis (mature)
Strictosidine aglycone	✓ Secondary phloem	✓ Pith, Xylem (Primary), Secondary phloem (Secondary)	✓ Mesophyll, phloem (Old)	✓ Epidermis, Pedicel
Isorauhimbine	✓ Secondary phloem	✓ Xylem, Cortex, Secondary phloem (secondary)	✓ Phloem, Mesophyll	✓ Epidermis, Pedicel
RPI2	✓ Phelloderm	✓ Epidermal region (primary), xylem (primary), Secondary phloem (secondary)	✓ Phloem (Old)	✓ pedicel (Old)
RPI3	✓ Secondary phloem	✓ Xylem, secondary phloem (secondary), cortex (secondary)	✓ Phloem, Mesophyll	✓ Epidermis, Pedicel
RPI5	×	✓ Secondary phloem (secondary)	×	×
RPI4	✓ Secondary phloem	✓ Pith, secondary phloem (secondary)	✓ phloem (Old MALDI), Mesophyll (DESI)	✓ Epidermis, Pedicel
RPI6	✓ Secondary phloem	✓ Xylem, secondary phloem (secondary), cortex (secondary)	✓ Phloem, Mesophyll	✓ Epidermis, Pedicel
RPI7	×	✓ Epidermal-suber area	✓ Phloem, Mesophyll	✓ Pedicel
Reserpine	✓ Secondary phloem, phelloderm, cork, xylem	✓ several areas in the tissue	✓ Phloem (Old)	✓ Pericarp, Seed (immature)

uncertain whether it is actually present in fruit tissue. This could indicate that it does not accumulate in fruit tissue due to rapid conversion and that perhaps the conversion is slower in the pedicel. RPI5 was not observed in any of the fruit tissues, and RPI7 was only observed in the pedicel of mature and immature fruit tissue, which could have the same explanation as for RPI2.

Reserpine, on the other hand, was detected in the pericarp of both mature and immature fruit tissue. In some images of young fruit tissues, reserpine was found to be present in the seed, which could indicate reserpine is either synthesized in or transported to the seed during the maturation of the fruit.

Overall, the present study presents several novel findings compared to the previously published MSI work on *R. tetraphylla* by Kumara et al. (2019), owing among other factors to the difference in instrumentation with regards to spatial resolution, selectivity and sensitivity. In particular, the main MIA precursor, strictosidine, was detected in most MSI analyses in this study unlike in the study by Kumara et al. where strictosidine was not detected at all. Reserpine was observed by Kumara et al. in the in root and stem tissue, where it was mostly observed in pith tissue of roots. In this work, the root tissue did not have any pith region, which could be due to the young age the plants. Besides the lack of pith in the MS images in this work (Fig. 3), the distribution in root tissue is similar to the findings in the previous study.

2.5. Feeding experiments with tryptamine-d4

In order to further investigate the proposed biosynthetic intermediates of reserpine and rescinnamine, tryptamine-d4 was administered to roots, with the aim of determining whether the proposed metabolites were found in their d4-labelled versions, as this would indicate that the compounds are formed from tryptamine and potentially be parts of the biosynthetic pathway. The *m/z* values of the relevant d4-labelled intermediates are found in Table 1.

Among the various metabolites and intermediates, only strictosidine and reserpine were observed in their deuterium labelled versions; importantly, these two d4-labelled compounds were not detected in control root tissue not administered tryptamine-d4 (Fig. S5). Since it is already well established that tryptamine is efficiently incorporated into strictosidine and all MIAs, colocalisation of strictosidine and strictosidine-d4 signals further confirm molecular identity of these *m/z* values (St-Pierre et al., 2013). The reason for the lack of detectable d4-labelled intermediates may be that the accumulated amounts were too low. The amounts may be increased in future experiments by increased the amount of administered tryptamine-d4.

A similar labelling experiment was carried out with young leaves; the results from this experiment are shown in Fig. 9. As seen in Fig. 9, almost no ions corresponding to d4-labelled molecules were detected in the unlabeled control leaf tissue. Only strictosidine aglycone was observed both as unlabeled and d4-labelled in the control leaves. This signal from strictosidine-aglycone-d4 must therefore be ascribed to an interfering ion which is not related to the MIAs. In both labelled and unlabeled leaves, strictosidine was observed in the mesophyll area (Fig. 9), similar to what was found in Fig. 6D, and in addition, strictosidine-d4 was observed to have the same distribution in leaves administered tryptamine-d4.

Likewise, unlabeled isorauhimbine was observed both in labelled and control leaves, but isorauhimbine-d4 was only observed in leaves administered tryptamine-d4. Isorauhimbine-d4 was mainly observed in the mesophyll but to a limited extent also around the phloem and xylem in the midrib, whereas unlabeled isorauhimbine was observed in the midrib in the same abundance as in the mesophyll. This could be due to isorauhimbine being initially biosynthesized in mesophyll and subsequently accumulated in the midrib, or the signal in the midrib could potentially come from another interfering compound of the same *m/z* value.

RPI2-d4, RPI4-d4 and RPI5-d4 were not detected in the leaf tissue that had absorbed tryptamine-d4, and it is therefore not possible to prove their link to tryptamine. Non-labelled RPI2 and RPI5 were detected in leaves treated with tryptamine and tryptamine-d4; this could be stress induced, as they were not observed in the untreated young leaves (Fig. 6). Stress could have arisen from the leaves being excised from the plant.

Ions corresponding to RPI3-d4/RPI6-d4 and RPI7-d4 were detected in the mesophyll outside the midrib. This is in contrast to the non-labelled ions of RPI3/RPI6 and RPI7 that were detected in the phloem and xylem in the midrib as well. Ions corresponding to reserpine-d4 were not detected in leaves treated with tryptamine-d4. It is thus inconclusive whether leaf tissue has the ability to biosynthesize reserpine, even though unlabeled reserpine is vaguely detected in leaf tissue. In conclusion, the precursor experiment has shown that some of the *m/z* values are related to tryptamine and that the mesophyll plays a vital role in MIA biosynthesis in young leaves of *R. tetraphylla*.

Analysis of the MIA biosynthesis in leaves of *C. roseus* has shown that the seco-iridoid pathway takes place in the internal phloem associated parenchyma and epidermis cells, and metabolism into MIAs takes place in epidermis, idioblast and laticifer cells (de Bernonville et al., 2015;

Miettinen et al., 2014). In the present study of *R. tetraphylla* neither reserpine, rescinnamine nor their theoretical intermediates were proven to be present in these afore mentioned cells types, but instead found in the mesophyll and the phloem. Some compounds were more restricted than others, i.e. strictosidine in young leaf tissue, which was not observed in veins or midrib, and RPI7 in old leaf tissue, which was only observed in the mesophyll.

2.5.1. Detection of a potentially novel MIA in R. tetraphylla

In analysis of the MALDI-MSI data from the experiment on the young and old leaves, distinct images could be created of ions with masses *m/z* 825.40692 and *m/z* 863.36280 (±5 ppm), corresponding to protonated and potassium adducts of an unknown compound with the molecular formula $C_{46}H_{56}N_4O_{10}$ (Fig. S7). This is the same molecular formula as the MIA vincristine, which is a dimeric alkaloid deriving from catharanthine and vindoline and found in *C. roseus* (de Bernonville et al., 2015). Vincristine is not known to be produced in *Rauvolfia* sp., but in various online libraries (Metlin, ChEBI, HMDB & BraChemDB) no other compound matches the exact mass as vincristine within 5 ppm mass accuracy. The signals were observed in compartments in leaf tissue of *R. tetraphylla*, which could suggest its presence in idioblast or laticifer cells. Idioblast and laticifer cells are also where intermediates of vincristine are observed in leaf tissue of *C. roseus* (Burlat et al., 2004; Roepke et al., 2010; Yamamoto et al., 2019). To investigate this, MS/MS analysis was performed of a vincristine standard and a methanol extract of a *R. tetraphylla* leaf. The MS/MS analysis resulted in two different fragmentation patterns, thus confirming that the detected compound was not vincristine (Fig. S6). In the experiment where d4-labelled tryptamine was administered to a *R. tetraphylla* leaf, ions corresponding to $[C_{46}H_{52}N_4O_{10}D_4+H]^+$ were observed in young leaves treated with tryptamine-d4 (Fig. S7). This indicates that the compound derives from tryptamine and increases the likelihood that it is indeed a MIA. Although the ions observed in these MS analyses are not of vincristine, it could be a novel, dimeric alkaloid that is isomeric to vincristine. Vincristine is a chemotherapeutic drug, which has seen a shortage in recent times (Rabin, 2019); it would thus be highly beneficial if this new, unidentified MIA of the same molecular formula turned out to have similar pharmacological properties and could be used as a substitute or supplement for vincristine.

3. Conclusions

The use of high-resolution MALDI-MSI on a high-resolution mass spectrometer like the QExactive Orbitrap has enabled mapping of intermediates in the reserpine biosynthesis in root, stem, leaf and berry of *R. tetraphylla* at unsurpassed detail level and compound selectivity, identifying the location of several theoretical intermediates.

In order to test whether the proposed biosynthetic pathway for reserpine proceeds via the proposed intermediates, roots and leaves from the plant were administered deuterium labelled tryptamine. Subsequently, several of the intermediates were observed in their unlabeled as well as their labelled version. By analysing the produced data, it was also possible to discover a novel molecule in *R. tetraphylla*, which shares the exact same mass as the chemotherapeutic drug, vincristine. The molecule was confirmed not to be vincristine, but likely a different and previously undescribed dimeric alkaloid.

MSI results on their own are typically not enough to assess whether the different metabolites have been produced at the sites where they were detected or if they were transported there, but together with immunohistochemical localization of enzymes, it provides a much deeper understanding of where and how the biosynthesis takes place in the plant. This is important information, for example for determining which part of the plant to examine by transcriptomics when the aim is refactoring of plant biosynthesis in bacteria or yeast. Indeed, this is of particular importance for a plant like *R. tetraphylla*, which produces high-value compounds but only at limited availability.

4. Experimental

4.1. Plant samples for mass spectrometry imaging

Rauvolfia tetraphylla plants were grown from seeds (Konstanz botanical garden, Germany) in greenhouses, at 22–34 °C and 31–86% relative humidity. Plants varied in ages depending on which part was collected. Root samples were ca. Four months old, primary stem tissue were ca. Six months old, and secondary stem samples were ca. Ten months old at the time of harvest. Leaf samples were acquired as "old" and "young" leaves of plants at the age of ca. 12 months. "Old leaves" refers to the leaves first produced by the plant, thus they are some of the largest and most mature leaves. "Young leaves" refers to those on the very tip of the branch, thus they are some of the smallest and least mature leaves. Fruit samples were acquired as immature and mature from a plant age of 12–15 months. Immature fruits were green and had a smooth surface. Mature fruits had changed from green to a dark purple color and had a wrinkled surface.

4.2. Tryptamine-d4 absorption in roots

Seven months old *R. tetraphylla* plants were carefully up-rooted and rinsed for excess soil. Then, pieces of side-root of approx. 15 mm length were cut with a razor blade and placed in 1.5 mL Eppendorf tubes containing 150 μL 1 mM tryptamine-d4 (labelled at the two CH_2 groups, T894602, Toronto Research Chemicals). The roots absorbed the solvent for 30–40 min until the entire volume was absorbed. Then, the lower 1–1.5 cm of the root (from the tip) were cut and left in the closed Eppendorf tube overnight at room temperature. The next day, the roots were snap frozen in liquid nitrogen and prepared for MALDI-MS imaging.

4.3. Tryptamine-d4 absorption in leaves

Young leaves of *R. tetraphylla* were collected and placed individually in 10 μL 1 mM tryptamine-d4 solution in 5 mL Eppendorf tubes. The tubes were closed and the leaves were set to absorb overnight at room temperature. The next day, the leaves were snap frozen in liquid nitrogen and prepared for MALDI-MS imaging.

4.4. MALDI-MSI - sample preparation

Samples were harvested and placed in 50 mL falcon tubes and immediately suspended into liquid nitrogen for snap freezing. For root samples, the plants were uprooted and washed with tap water to remove the excess dirt before snap freezing. Samples were stored at −80 °C until further preparation.

Cryo-sectioning of samples was performed based on the methods developed by Kawamoto (Kawamoto, 2003; Kawamoto and Kawamoto, 2021) and adapted to plant samples by Montini et al. (2020), but with some modifications. A slurry of n-heptane and dry ice was prepared in a Dewar jar. A 2.5 × 2.0 cm mold (SECTION-LAB Co. Ltd.) was filled with 2% (wt/v) aqueous gel of carboxymethyl cellulose and immersed in the n-heptane dry ice slurry, but not submerged. When the edges of the embedding media were starting to freeze, the sample was placed in the embedding media, and the mold was carefully submerged in the n-heptane until frozen. The frozen block was removed from the mold and stored at −80 °C until cryo-sectioning. Embedded plant samples were cryo-sectioned at −23 °C using a LEICA CM3050S cryo-microtome (Leica Microsystems, Wetzlar Germany). Using the cryo-microtome, the embedded sample was trimmed to the desired section of the sample. Cross sections of the leaves were taken approximately from the longitudinal center of the leaf. To achieve 10 μm sections of the plant tissue, cryo-film (SECTION-LAB Co. Ltd. Hiroshima, Japan) was adhered to the sample prior to sectioning. Once sectioned, the opposite side of the cryo-films were fixated to glass-slides using double-sided carbon tape

(Electron Microscopy Sciences, Hatfield, PA, USA) and stored at −80 °C until the MALDI imaging experiment.

Prior to matrix application, cryo-sectioned samples were freeze-dried overnight. Subsequently, optical images of the plant samples were taken using an Olympus BH-2 microscope with reflected light. 2,5-dihydroxybenzoic acid (DHB, Merck Danmark, Søborg) was used as MALDI matrix and applied to samples using an in-house built pneumatic matrix sprayer. The spraying parameters were as follows: 300 μL of 30 mg/mL DHB dissolved in MeOH/H_2O (90:10) was sprayed at a flow rate of 30 μL/min from a distance of 11 cm to the sample, using a nebulizing gas pressure of 2 bar while the sample was rotating at a speed of 600 rpm.

4.5. MALDI MSI - analysis

MALDI-MSI was performed on a Thermo QExactive Orbitrap mass spectrometer equipped with an AP-SMALDI5 ion source (TransMIT GmbH, Giessen, Germany). Spectra were acquired in positive ion mode with a scan range of *m/z* 150–1050, at mass resolving power 140,000 at *m/z* 200. Two matrix peaks of DHB were used as lock masses (*m/z* 431.0374 and *m/z* 721.0800). The pixel size varied between samples, as specified with the presented images.

4.6. DESI-MSI - sample preparation

Leaf tissue of *R. tetraphylla* was imprinted on porous PTFE, as described elsewhere (Thunig et al., 2011). Briefly, using a vise the abaxial side of the leaf was pressed towards a piece of porous PTFE together with a piece of tissue paper to absorb excess liquid. After 10–15 s of pressure, the pressure was lifted, and the PTFE imprint was ready for analysis by DESI-MSI. Old – and thus very large – leaves were separated into several sections, imaged individually and merged into a single MS-image.

4.7. DESI MSI - analysis

DESI-MSI was performed on a Thermo QExative Orbitrap mass spectrometer (Thermo Scientific, Bremen, Germany) equipped with a custom built DESI-MSI ion source (Thunig et al., 2011). Spectra were acquired in positive ion mode (scan range: *m/z* 150–1050) at mass resolving power 140,000 at *m/z* 200. The peak from diisooctyl phthalate ($[C_{24}H_{38}O_4 + Na]^+$, *m/z* 413.2662), a common contaminant in the background, was used as lock mass.

4.8. Data analysis

Raw data files from DESI- and MALDI-MSI experiments were converted to imzML files (Schramm et al., 2012) using the "RAW + UDP to IMZML" software (v1.6R170; TransMIT, Bremen, Germany), and MS images were generated using MSiReader v1.01 (Bokhart et al., 2018) using a mass tolerance of 5 ppm. All MS images were normalized to the Total Ion Current (TIC) and the color scale was adjusted to provide the best possible representation of the compounds of interest. Every MS image of reserpine, rescinamine and their intermediates are summed images of *m/z* values corresponding to the protonated analytes as well as their sodium and potassium adducts (Table 1). Two primary metabolites, phosphatidylcholine 34:2 (PC (34:2)) ($[C_{42}H_{80}NO_8P + K]^+$, *m/z* 796.52532) and di-hexose ($[C_{12}H_{22}O_{11} + K]^+$, *m/z* 381.07937) were used as tissue markers to show the contours of the tissue. All the presented MS-images have been reproduced with $N = 2$ biological replicates, and the presented images are representative of both experiments.

4.9. MS/MS analysis

Leaves of *R. tetraphylla* were freeze-dried overnight and manually mortared to a fine powder. 120 mg leaf powder was extracted in 1 mL of methanol by sonication for 45 min and centrifuged for 10 min at 1120 g. The supernatant was filtered through a 0.22 μm filter (CA syringe filter, Frisenette) prior to analysis. A standard of vincristine (purchased at Merck) was dissolved in methanol to a concentration of 10 ppm.

MS/MS analysis was performed on a Thermo LTQ linear ion trap mass spectrometer. The leaf extract and the vincristine standard were analyzed by electrospray ionization at a flow rate of 5 μL/min using a collision energy of 22 (arb. units).

Short summary

Comprehensive mapping of intermediates in the reserpine pathway was performed by mass spectrometry imaging in root, stem, leaf and fruit tissue of *R. tetraphylla*.

Declaration of competing interest

The authors declare that they have no known competing financial interests or personal relationships that could have appeared to influence the work reported in this paper.

Data availability

Raw data in form of imzML files of the presented data has been uploaded to the Metaspace platform (https://nam11.safelinks.protection.outlook.com/?url=https%3A%2F%2Fmetaspace2020.eu%2F&data=05%7C01%7Ca.hubertt%40elsevier.com%7Cb6203f21d30a47ef718208db1be01a2e%7C9274ee3f94254109a27f9fb15c10675d%7C0%7C0%7C638134422277796011%7CUnknown%7CTWFpbGZsb3d8eyJWIjoiMC4wLjAwMDAiLCJQIjoiV2luMzIiLCJBTiI6Ik1haWwiLCJXVCI6Mn0%3D%7C3000%7C%7C%7C&sdata=XXoxPWucapCWBrVkrf4DmXJk93m%2B7pC6U%2FjlVisa4Og%3D&reserved=0) (Palmer et al., 2017) from where it is freely available.

Acknowledgements

This research was funded by the EU Horizon 2020 research and innovation program (MIAMi project grant agreement No. 814645). Support for MALDI imaging instrumentation from the Carlsberg Foundation and The Danish Council for Independent Research|Medical Sciences (grant no. DFF – 4002–00391) is gratefully acknowledged. Illustrations were drawn by Debbie Maizels, Zoobotanica Scientific Illustration. N.B. was supported by a grant from the VILLUM Foundation, Denmark (grant no. 19151).

Appendix A. Supplementary data

Supplementary data to this article can be found online at https://doi.org/10.1016/j.phytochem.2023.113620.

References

Babu, N.C., Naidu, M.T., Venkaiah, M., 2010. Ethnomedicinal plants of Kotia hills of Vizianagaram district, Andhra Pradesh, India. J. Phytol. 2, 76–82.
Bakris, G.L., Frohlich, E.D., 1989. The evolution of antihypertensive therapy: an overview of four decades of experience. J. Am. Coll. Cardiol. 14, 1595–1608.
Baratto, L.C., Duarte, M.d.R., Santos, C.A.d.M., 2010. Pharmacobotanic characterization of young stems and stem barks of Rauvolfia sellowii. Müll. Arg., Apocynaceae. Braz. J. Pharm. Sci. 46, 555–561.
Bjarnholt, N., Li, B., D'Alvise, J., Janfelt, C., 2014. Mass spectrometry imaging of plant metabolites – principles and possibilities. Nat. Prod. Rep. 31, 818–837.
Bokhart, M.T., Nazari, M., Garrard, K.P., Muddiman, D.C., 2018. MSiReader v1.0: evolving open-source mass spectrometry imaging software for targeted and untargeted analyses. J. Am. Soc. Mass Spectrom. 29, 8–16.
Boughton, B.A., Thinagaran, D., Sarabia, D., Bacic, A., Roessner, U., 2016. Mass spectrometry imaging for plant biology: a review. Phytochemistry Rev. 15, 445–488.
Burlat, V., Oudin, A., Courtois, M., Rideau, M., St-Pierre, B., 2004. Co-expression of three MEP pathway genes and geraniol 10-hydroxylase in internal phloem parenchyma of Catharanthus roseus implicates multicellular translocation of intermediates during the biosynthesis of monoterpene indole alkaloids and isoprenoid-derived primary metabolites. Plant J. 38, 131–141.

Court, W., Evans, W., Trease, G., 1957. The structure of the root and stem of rauwolfia caffra sond. J. Pharm. Pharmacol. 9, 237–250.
Dalisay, D.S., Kim, K.W., Lee, C., Yang, H., Rubel, O., Bowen, B.P., Davin, L.B., Lewis, N. G., 2015. Dirigent protein-mediated lignan and cyanogenic glucoside formation in flax seed: integrated omics and MALDI mass spectrometry imaging. J. Nat. Prod. 78, 1231–1242.
Dang, T.-T.T., Franke, J., Carqueijeiro, I.S.T., Langley, C., Courdavault, V., O'Connor, S. E., 2018. Sarpagan bridge enzyme has substrate-controlled cyclization and aromatization modes. Nat. Chem. Biol. 14, 760–763.
Dang, T.T.T., Franke, J., Tatsis, E., O'Connor, S.E., 2017. Dual catalytic activity of a cytochrome P450 controls bifurcation at a metabolic branch point of alkaloid biosynthesis in Rauwolfia serpentina. Angew. Chem. 129, 9568–9572.
de Bernonville, T.D., Clastre, M., Besseau, S., Oudin, A., Burlat, V., Glévarec, G., Lanoue, A., Papon, N., Giglioli-Guivarc'h, N., St-Pierre, B., 2015. Phytochemical genomics of the Madagascar periwinkle: unravelling the last twists of the alkaloid engine. Phytochemistry 113, 9–23.
Deshmukh, S.R., Ashrit, D.S., Patil, B.A., 2012. Extraction and evaluation of indole alkaloids from Rauwolfia serpentina for their antimicrobial and antiproliferative activities. Int. J. Pharm. Pharmaceut. Sci. 4, 329–334.
Elisabetsky, E., Costa-Campos, L., 2006. The alkaloid alstonine: a review of its pharmacological properties. Evid. base Compl. Alternative Med. 3, 39–48.
Feenstra, A.D., Dueñas, M.E., Lee, Y.J., 2017. Five micron high resolution MALDI mass spectrometry imaging with simple, interchangeable, multi-resolution optical system. J. Am. Soc. Mass Spectrom. 28, 434–442.
Fife, R., Maclaurin, J., Wright, J., 1960. Rescinnamine in treatment of hypertension in hospital clinic and in general practice. Br. Med. J. 2, 1848.
Ganesh, P., Sudarsanam, G., 2013. Ethnomedicinal plants used by yanadi tribes in seshachalam biosphere reserve forest of chittoor district, Andhra Pradesh India. Int. J. Pharm. Life Sci. 4, 3073–3079.
Gupta, S., Khanna, V.K., Maurya, A., Bawankule, D.U., Shukla, R.K., Pal, A., Srivastava, S. K., 2012. Bioactivity guided isolation of antipsychotic constituents from the leaves of Rauwolfia tetraphylla L. Fitoterapia 83, 1092–1099.
Iqbal, A.A.M., Khan, F.A.K., Khan, M., 2013. Ethno-phyto-pharmacological overview on Rauwolfia tetraphylla L. Int. J. Pharm. Phytopharmacol. Res. 2, 247–251.
Kawamoto, T., 2003. Use of a new adhesive film for the preparation of multi-purpose fresh-frozen sections from hard tissues, whole-animals, insects and plants. Arch. Histol. Cytol. 66, 123–143.
Kawamoto, T., Kawamoto, K., 2021. Preparation of Thin Frozen Sections from Nonfixed and Undecalcified Hard Tissues Using Kawamoto's Film Method (2020). Skeletal Development and Repair. Springer, pp. 259–281.
Klohs, M., Draper, M., Keller, F., 1954. Alkaloids of Rauwolfia serpentina Benth. iii. 1 rescinnamine, a new hypotensive and sedative principle. J. Am. Chem. Soc. 76, 2843-2843.
Kumar, S., Sankaranarayanan, S., Bama, P., Baskar, R., Kanagavalli, K., 2018. An ethnobotanical study of medicinal plants used by local people and tribals in Topslip (Annamalai hills) and Ooty (Chinchona village) of Coimbatore and Ooty district. Int. J. Curr. Res. 10, 69304–69308.
Kumar, S., Singh, A., Bajpai, V., Srivastava, M., Singh, B.P., Kumar, B., 2016. Structural characterization of monoterpene indole alkaloids in ethanolic extracts of Rauwolfia species by liquid chromatography with quadrupole time-of-flight mass spectrometry. J. Pharm. Anal. 6, 363–373.
Kumara, P.M., Shaanker, R.U., Pradeep, T., 2019. UPLC and ESI-MS analysis of metabolites of Rauvolfia tetraphylla L. and their spatial localization using desorption electrospray ionization (DESI) mass spectrometric imaging. Phytochemistry 159, 20–29.
Li, B., Bhandari, D.R., Römpp, A., Spengler, B., 2016. High-resolution MALDI mass spectrometry imaging of gallotannins and monoterpene glucosides in the root of Paeonia lactiflora. Sci. Rep. 6, 1–12.
Mahalakshmi, S., Achala, H., Ramyashree, K., Prashith Kekuda, T., 2019. Rauvolfia tetraphylla L.(Apocynaceae)-a comprehensive review on its ethnobotanical uses, phytochemistry and pharmacological activities. Int. J. Pharm. Biol. Sci. 9, 664–682.
Malaiya, P.S., 2016. Medicinal plants used by tribal population of Anuppur district Madhya Pradesh, India. Int. J. Appl. Res. 2, 418–421.
Metcalfe, C.R., Chalk, L., 1950. Anatomy of the Dicotyledons. In: Anatomy of the Dicotyledons, s. vols. 1 & 2.
Miettinen, K., Dong, L., Navrot, N., Schneider, T., Burlat, V., Pollier, J., Woittiez, L., Van Der Krol, S., Lugan, R., Ilc, T., 2014. The seco-iridoid pathway from Catharanthus roseus. Nat. Commun. 5, 1–12.
Montini, L., Crocoll, C., Gleadow, R.M., Motawia, M.S., Janfelt, C., Bjarnholt, N., 2020. Matrix-assisted laser desorption/ionization-mass spectrometry imaging of metabolites during sorghum germination. Plant Physiol 183, 925–942.
Morshed, A.J.M., Nandni, N.C., 2012. Indigenous medicinal plants used by the tribal healers of chittagong hill tracts to treat diarrhoea and dysentery. Hamdard Med. 55, 48–66.
Muller, J., Schlittler, E., Bein, H., 1952. Reserpin, the sedative principle from Rauwolfia serpentina B. Experientia 8, 338.
Mullin, S., Mani, N., Grossman, T.H., 2004. Inhibition of antibiotic efflux in bacteria by the novel multidrug resistance inhibitors biricodar (VX-710) and timcodar (VX-853). Antimicrob. Agents Chemother. 48, 4171–4176.
O'Connor, S.E., Maresh, J.J., 2006. Chemistry and biology of monoterpene indole alkaloid biosynthesis. Nat. Prod. Rep. 23, 532–547.
Palmer, A., Phapale, P., Chernyavsky, I., Lavigne, R., Fay, D., Tarasov, A., Kovalev, V., Fuchser, J., Nikolenko, S., Pineau, C., Becker, M., Alexandrov, T., 2017. FDR-controlled metabolite annotation for high-resolution imaging mass spectrometry. Nat. Methods 14, 57–60.
Pan, Q., Mustafa, N.R., Tang, K., Choi, Y.H., Verpoorte, R., 2016. Monoterpenoid indole alkaloids biosynthesis and its regulation in Catharanthus roseus: a literature review from genes to metabolites. Phytochemistry Rev. 15, 221–250.
Rabin, R.C., 2019. Faced with a Drug Shortfall, Doctors Scramble to Treat Children with Cancer (New York Times).
Roepke, J., Salim, V., Wu, M., Thamm, A.M., Murata, J., Ploss, K., Boland, W., De Luca, V., 2010. Vinca drug components accumulate exclusively in leaf exudates of Madagascar periwinkle. Proc. Natl. Acad. Sci. USA 107, 15287–15292.
Schramm, T., Hester, A., Klinkert, I., Both, J.-P., Heeren, R.M.A., Brunelle, A., Laprévote, O., Desbenoit, N., Robbe, M.-F., Stoeckli, M., Spengler, B., Römpp, A., 2012. imzML — a common data format for the flexible exchange and processing of mass spectrometry imaging data. J. Proteonomics 75, 5106–5110.
St-Pierre, B., Besseau, S., Clastre, M., Courdavault, V., Courtois, M., Creche, J., Ducos, E., de Bernonville, T.D., Dutilleul, C., Glevarec, G., 2013. Deciphering the evolution, cell biology and regulation of monoterpene indole alkaloids. Adv. Bot. Res. 68, 73–109. Elsevier.
St-Pierre, B., Vazquez-Flota, F.A., De Luca, V., 1999. Multicellular compartmentation of Catharanthus roseus alkaloid biosynthesis predicts intercellular translocation of a pathway intermediate. Plant Cell 11, 887–900.
Stavri, M., Piddock, L.J., Gibbons, S., 2007. Bacterial efflux pump inhibitors from natural sources. J. Antimicrob. Chemother. 59, 1247–1260.
Stöckigt, J., Panjikar, S., Ruppert, M., Barleben, L., Ma, X., Loris, E., Hill, M., 2007. The molecular architecture of major enzymes from ajmaline biosynthetic pathway. Phytochemistry Rev. 6, 15–34.
Thunig, J., Hansen, S.H., Janfelt, C., 2011. Analysis of secondary plant metabolites by indirect desorption electrospray ionization imaging mass spectrometry. Anal. Chem. 83, 3256–3259.
Treimer, J.F., Zenk, M.H., 1979. Purification and properties of strictosidine synthase, the key enzyme in indole alkaloid formation. Eur. J. Biochem. 101, 225–233.
Vaou, N., Stavropoulou, E., Voidarou, C., Tsigalou, C., Bezirtzoglou, E., 2021. Towards advances in medicinal plant antimicrobial activity: a review study on challenges and future perspectives. Microorganisms 9, 2041.
Verma, R.K., Gupta, S., Gupta, M.M., Srivastava, S.K., 2012. A simple isocratic HPLC method for the simultaneous determination of antipsychotic indole alkaloids in Rauwolfia tetraphylla. J. Liq. Chromatogr. Relat. Technol. 35, 937–950.
Yamamoto, K., Takahashi, K., Caputi, L., Mizuno, H., Rodriguez-Lopez, C.E., Iwasaki, T., Ishizaki, K., Fukaki, H., Ohnishi, M., Yamazaki, M., 2019. The complexity of intercellular localisation of alkaloids revealed by single-cell metabolomics. New Phytol. 224, 848–859.
Yamamoto, K., Takahashi, K., Mizuno, H., Anegawa, A., Ishizaki, K., Fukaki, H., Ohnishi, M., Yamazaki, M., Masujima, T., Mimura, T., 2016. Cell-specific localization of alkaloids in Catharanthus roseus stem tissue measured with Imaging MS and Single-cell MS. Proc. Natl. Acad. Sci. USA 113, 3891–3896.